

Article

Effect of the Acid-Etching on Grit-Blasted Dental Implants to Improve Osseointegration: Histomorphometric Analysis of the Bone-Implant Contact in the Rabbit Tibia Model

Blanca Ríos-Carrasco ¹, Bernardo Ferreira Lemos ², Mariano Herrero-Climent ³, F. Javier Gil Mur ^{4,5,*}
and Jose Vicente Ríos-Santos ¹

¹ Department of Periodontology, Dental School, University of Seville, 41009 Seville, Spain; brios@us.es (B.R.-C.); jvrios@us.es (J.V.R.-S.)

² Department of Dentistry and Medical Sciences, Faculty of Health Sciences, University Fernando Pessoa, 4249-004 Porto, Portugal; blemos@ufp.edu.pt

³ Department of Periodontology, Porto Dental Institute, 4150-518 Porto, Portugal; dr.herrero@herrerocliment.com

⁴ Bioengineering Institute of Technology, Facultad de Medicina y Ciencias de la Salud, Universitat Internacional de Catalunya, 08195 Sant Cugat del Vallés, Spain

⁵ Faculty of Dentistry, Universitat Internacional de Catalunya, 08195 Sant Cugat del Vallés, Spain

* Correspondence: xavier.gil@uic.es



Citation: Ríos-Carrasco, B.; Lemos, B.F.; Herrero-Climent, M.; Gil Mur, F.J.; Ríos-Santos, J.V. Effect of the Acid-Etching on Grit-Blasted Dental Implants to Improve Osseointegration:

Histomorphometric Analysis of the Bone-Implant Contact in the Rabbit Tibia Model. *Coatings* **2021**, *11*, 1426. <https://doi.org/10.3390/coatings11111426>

Academic Editor: Devis Bellucci

Received: 6 November 2021

Accepted: 20 November 2021

Published: 22 November 2021

Publisher's Note: MDPI stays neutral with regard to jurisdictional claims in published maps and institutional affiliations.



Copyright: © 2021 by the authors. Licensee MDPI, Basel, Switzerland. This article is an open access article distributed under the terms and conditions of the Creative Commons Attribution (CC BY) license (<https://creativecommons.org/licenses/by/4.0/>).

Abstract: Previous studies have shown that the most reliable way to evaluate the success of an implant is by bone-to-implant contact (BIC). Recent techniques allow modifications to the implant surface that improve mechanical and biological characteristics, and also upgrade osseointegration. **Objective:** The aim was to evaluate the osseointegration in rabbit tibia of two different titanium dental implant surfaces: shot-blasted with Al₂O₃ (SB) and the same treatment with an acid-etching by immersion for 15 s in HCl/H₂SO₄ (SB + AE). **Material and methods:** Roughness parameters (R_a, R_t, and R_z) were determined by white light interferometer microscopy. Surface wettability was evaluated with a contact angle video-based system using water, di-iodomethane, and formamide. Surface free energy was determined by means of Owens and Wendt equations. Scanning electron microscopy equipped with X-ray microanalysis was used to study the morphology and determine the chemical composition of the surfaces. Twenty-four grade 4 titanium dental implants (Essential Klockner®) were implanted in the rabbit's tibia, 12 for each surface treatment, using six rabbits. Six weeks later the rabbits were sacrificed and the implants were sent for histologic analysis. Resonance frequency analysis (RFA) was recorded both at the time of surgery and the end of the research with each device (Osstell Mentor and Osstell ISQ). **Results:** The roughness measurements between the two treatments did not show statistically significant differences. However, the effect of the acid etching made the surface slightly more hydrophilic (decreasing contact angle from 74.7 for SB to 64.3 for SB + AE) and it presented a higher surface energy. The bone-to-implant contact ratio (BIC %) showed a similar tendency, with 55.18 ± 15.67 and 59.9 ± 13.15 for SB and SB + AE implants, respectively. After 6 weeks of healing, the SB + AE showed an implant stability quotient (ISQ) value of 76 ± 4.47 and the shot-blasted one an ISQ value of 75.83 ± 8.44 (no statistically significant difference). Implants with different surface properties had distinctive forms of behavior regarding osseointegration. Furthermore, the Osstell system was an invasive and reliable method to measure implant stability. **Conclusion:** Both surfaces of implants studied showed high osseointegration. The SB and SB + AE implants used in our study had similar behavior both in terms of BIC values and RFA. The RFA systems in Osstell Mentor and Osstell ISQ confirmed nearly perfect reproducibility and repeatability.

Keywords: titanium surface; surface roughness; histomorphometric analysis; animal studies; resonance frequency analysis; implant stability

1. Introduction

Dental titanium implants are currently the method of choice to replace missing dental teeth. It is done via the process of osseointegration [1]. A successfully osteointegrated implant is defined by direct bone-to-implant contact (BIC) without the interposition of non-bone connective tissue [1–3]. Several parameters affect the percentage of BIC, such as the quality and quantity of the bone that surrounds the implant surface, macroscopic design, microscopic design, the prosthetic load to which the implant is subjected, the state of the patient, and more. The osteoblastic cell union and the newly immature bone created around the implant surface are guided by the adsorption proteins factors [4].

Recent publications show that the modification of the microsurface of the titanium (Ti) can improve the adhesion, proliferation, and differentiation of human osteoblasts and, as a consequence, osseointegration [5–7]. The roughness produces an increase in the surface in contact with the patient's native bone. Pure titanium and mixtures of it are extensively used in the dental implant field because of its noble mechanical properties and exceptional biocompatibility compared to other materials such as zirconium [5,6]. The studies reviewed compared titanium rough implant surfaces with a polished or machined surface, obtaining better results in the former in terms of faster bone integration, a more significant percentage of bone–implant contact, and resistance to shear [2,8].

During the osseointegration phenomenon, immature bone is created by the cells around the implant surface. Different methods to obtain surface roughness have been developed in titanium implants, as well as special techniques to improve chemistry and/or topography. These methods include anodization, grit blasting, sand blasting, acid etching, and a combination of these [4,8,9]. The most frequently used treatment for producing an irregular surface on a titanium dental implant is sandblasting. This method consists of projecting abrasive particles such as alumina (Al_2O_3) from the gun to the surface. This inorganic abrasive is biologically inert ceramic particles. It has been demonstrated that the alumina residual in the surface of around 7%–11% does not influence the osseointegration and no inflammatory reactions have been observed [10,11].

The variation of the surface roughness of dental implants from around 1.5 to 3.5 micrometers significantly influences the osteoblast cell behavior in vitro and this increase in roughness improves the surface free energy, increasing the reactivity. These surface properties also produce an improvement in the long-term in vivo response, increasing the quantity of bone in direct contact with the implant surface as well as the loads and torsion moments required for the movement of the dental implant from the bone [2,12].

An appropriate osseointegration requests the adhesion of proteins to the roughness of the implant surface, and the osteoblastic actuation needs fibronectin and vitronectin. Nowadays, a rough implant surface (S_a) of 1 to 2 μm has faster osseointegration than a surface with less roughness (S_a of 0.5 to 1 μm) [13].

On the other hand, it is agreed that implant primary stability has a relevant role in the long-term success of dental implants. A quantitative method is required for the measurement of implant stability and osseointegration [14]. Resonance frequency analysis (RFA), which was introduced by Meredith, has been proposed as a non-invasive and non-destructive means to measure implant integration and detect stability changes over time [15,16] and assist in preventing osseointegration failures that show reduced stability over time [17]. The increase/decrease at the implant-to-bone interface in healing variations can be measured and registered by resonance frequency analysis (RFA) [17,18].

One of the most-used clinical tools is currently the Osstell instrument (Gothenburg, Sweden), which allows the initial stability of the implant to be evaluated, as well as the progression of that ISQ, which allows for a predictable loading protocol [17]. This technique can measure the initial stability of an implant in a nondestructive manner, unlike histomorphometric analysis, which provides considerable information, but can be used only in animal studies [19,20].

Various types of clinical evaluation of RFA have emerged in the last few years: Osstell AB (the first generation), Osstell Mentor (the second), and Osstell ISQ (the third)

provide excellent clinical results [14]. Currently, the development of this system has guided different companies to use RFA. RFA is an “almost perfect” method in terms of reproducibility and repeatability, and is very reliable, universal, innocuous, simple, and widely available [17,20].

The animal model selected (white New Zealand rabbits) is currently one of the most used, and many studies have guaranteed their usefulness [13,18]. The surgical technique was described by Johansson and Albrektsson in 1987 and was an essential part of investigation before human studies [14]. Earlier findings show that in the tibia model, the implant is placed in contact almost exclusively with the cortical bone and that the bone creation is distributed in two phases: (1) around the cortical portion of the implant (first and second threads) and (2) around the intramedullary portion of the screw (third and fourth threads) [12].

The aim of the present histomorphometric study was to evaluate the effect of acid-etching after shot-blasting osseointegration implants. Two types of surfaces were implanted in the tibiae epiphyses of rabbits, and the correlation between the BIC percentage and RFA values was analyzed. The second objective of the study was to compare the reliability of two generations of analysis frequency devices (Osstell Mentor and Osstell ISQ).

2. Materials and Methods

2.1. Materials

The dental implants used were Klockner Essential Cone (SOADCO, Escaldes Engordany, Andorra) with dimensions of 4.0 mm × 8.0 mm per implant and a neck section that was 1.5 mm (Figure 1). The implant is made with commercially pure Titanium grade 4.



Figure 1. Essential Cone dental implant.

Two different surfaces were used:

1. SB: shot-blasted with Al_2O_3 particles of 425 to 600 mm. The surface roughness was made at 0.25 MPa, washed on ultrasound for 10 min with soap, and dried with forced air.
2. SB + AE: The same treatment of SB followed by acid etching with a combination of HCl/ H_2SO_4 at 40 °C for 3 min.

2.2. Measurements of Roughness

The determination of the surface roughness of the dental implants was measured by means of white light interferometry (WLI) equipment (Optical Profiling System, Wyko NT9300, Veeco Instruments, Plainview, NY, USA). This equipment allows for measurements of 3D structures by using a wave superposition principle with a visible-wavelength light (white light). Seven areas were selected on the different parts of the implant surface, and the average of each parameter evaluated was calculated with Wyko Vision 232™ Software (Veeco Instruments, Plainview, NY, USA).

The roughness parameters studied were R_a , defined as the arithmetical mean roughness height, indicating the average of the absolute value along the sampling length; R_t , defined as the vertical distance between the maximum profile peak height and the maximum profile valley depth along the evaluation length; and R_z , which indicates the absolute vertical distance between the maximum profile peak height and the maximum profile valley depth along the sampling length [5,7,10].

2.3. Wettability and Surface Energy

Surface wettability was evaluated with a contact angle video-based system (Contact Angle System OCA15plus, Dataphysics, Santa Clara, CA, USA) and analyzed with proprietary software (SCA20, Dataphysics, Filderstat, Germany). All the experiments were performed under a controlled temperature and 100% relative humidity. Static contact angles (CA) of three reference liquids (ultrapure distilled water (MilliQ-Merck, Darmstadt, Germany), di-iodomethane, and formamide) were measured by the sessile drop method. The drops were dispensed on the substrate surface under controlled temperature ($T = 25\text{ }^{\circ}\text{C}$) and 100% relative humidity. The wettability was studied with the help of a contact angle goniometer (OCA 15+, Dataphysics, Filderstat, Germany).

Total surface free energy (SFE), the “London” or “dispersion” component, and the “polar” component of SFE for all series were calculated after CA was measured with two different liquids on each material: ultrapure distilled water (MilliQ) and di-iodomethane. The SFE and its components were obtained by means of the Owens and Wendt equation [21,22].

$$\gamma_S = \gamma_S^d + \gamma_S^p \quad (1)$$

$$\gamma_L(1 + \cos \theta) = 2((\gamma_L^d \times \gamma_S^d)^{1/2} + (\gamma_L^p \times \gamma_S^p)^{1/2}) \quad (2)$$

where γ_L^d is the dispersive part of the liquid surface tension and γ_L^p is the polar part of the liquid surface tension. θ is the contact angle of the liquid L and solid S.

2.4. Evaluation of the Surface Chemical Composition

Elemental chemical composition on the surface was measured by means of electron spectroscopy for chemical analysis (ESCA), also denominated X-ray photoelectron spectroscopy (XPS) (Physical Electronics, Chanhansen, NN, USA). The ESCA method measures the energy detected of photoelectrons generated at the surface by X-ray radiation. This technique allows the chemical elements present on the metallic surfaces to be determined both qualitatively and quantitatively. Only two elements are not detectable: hydrogen and helium.

2.5. Surgical Procedure

For this study, six male rabbits were used. A total of 24 dental implants (Section 2.1) were placed in both tibiae of 6 white New Zealand rabbits of 6 months of age weighing 3000 to 4000 g. This study was approved by the Animal Research Committee of Seville University and the Ethical Committee of the University of Cordoba (Reference 2041/PI11). All the implants were placed according to the surgical procedure indicated by the implant system.

The resonance frequency analysis (RFA) was measurement (at the implant procedure and after sacrifice):

- Osstell Mentor II (second generation) (Gothenburg, Sweden).
- Osstell ISQ (third generation) (Gothenburg, Sweden).

This system was chosen because it is non-invasive, records the primary stability, assesses the evolution, and is objective, reproducible, and repeatable.

The surgical procedures included an anesthesia protocol that began with premedication with acepromazine IM (maximum 0.1 mg/kg). General anesthesia included ketamine (5 to 8 mg/kg IV), acepromazine (0.5 to 1 mg/kg), and atropine (0.05 mg/kg). Amoxicillin IM was administered at the end of surgery (0.1 mL/kg).

Two dental implants were inserted randomly in the proximal metaphyseal area of both tibiae. The procedures during the surgery were performed in accordance with brand guidelines for implantation. After implant placement, RFA values were recorded for each implant (Osstell[®] Integration Diagnostics, Savedalen, Sweden) as well as ISQ values (three times for each implant with Osstell Mentor II and two times for each implant with Osstell ISQ), cover screws were placed, and finally the rounds were closed with resorbable sutures.

Postoperative care included antibiotics (enrofloxacin 5 mg/kg IM every 24 h for 7 days) and pain control (meloxicam 0.1 mg/kg every 24 h). During this interval, all rabbits were maintained on a normal diet and given water ad libitum.

After that, 42 days later, all animals were sedated, the cover screws were removed, and RFA values were recorded for each implant (in the same way as the surgery placement). At that time, the animals were sacrificed by means of an intracardiac overdose of thiopental.

2.6. Implant Stability Measurements (ISQ)

Primary stability was obtained for all implants using two different resonance frequency analyzers (Osstell Mentor II and Osstell ISQ) (Osstell™, Integration Diagnostics AB, Gothenburg, Sweden). First, the measurements were obtained using the second-generation resonance frequency analyzer (Osstell Mentor II), and after that Osstell ISQ was used. The cover screw was removed, and a transducer (magnetic peg) (Smartpeg, Integration Diagnostics AB, Göteborg, Sweden) was attached in a buccal–lingual direction, perpendicular to the bone. The measurement was taken three times for Osstell Mentor II and twice for Osstell ISQ, and the ISQ values were recorded.

2.7. Histological and Histomorphometric Analyses

Specimens were fixed in 4% formaldehyde neutral solution, dehydrated in graded series of ethanol (70%, 80%, 96%, and 100%), and embedded first in a preparation of 50% alcohol and 50% acrylic resin light curing and in a second stage in 100% polymethyl methacrylate (Technovit 7200VLC, Zülzer, Bonn, Germany). Masson-Goldner staining analysis was performed. The samples were polymerized with a control light and external cooling unit (Exact 520-530, Exakt Apparatebau GmbH, Norderstedt, Germany). Each implant was longitudinally sectioned in the middle with a circular diamond saw (Exact 300-310, Exakt Apparatebau GmbH, Norderstedt, Germany). After that, the surfaces of the blocks were polished and sputter coated. The sections were then ground to a final thickness of about 30 µm. Later on, they were grinded and polished with SiC abrasive paper of P400, P800, and P1200 and likewise for the control (Exact 400CS, Exakt Apparatebau GmbH, Norderstedt, Germany).

Global histomorphometry was carried out using a program developed in an image-processing system (Zeiss Axio, Axio, New York, NY, USA). The percentage of direct contact between mineralized bone and the titanium surface was calculated using IMAGE J software 1.43 (Wayne Rasband—National Institutes of Health, Bethesda, MD, USA). The final results of the amount of bone were obtained by a modified formula of bone–implant contact: partial BIC (pBIC)—the percentage of bone-to-implant contact retrieved divided by the bone of the tibia prior to the surgery, on each image of each implant.

A scanning electron microscope (SEM) (JSM 6400, Jeol, Tokyo, Japan) was used to qualitatively analyze the surface topography. This microscope is equipped with X-ray diffractometer EDX microanalysis in order to determine the chemical composition on the surfaces.

2.8. Statistical Analysis

The minimal sample size was designed for the comparison of two independent means with nQuery Advisor® (Version 7.0), taking into account a two-sided 5% level of significance, a 0.80 power to detect a significant difference, a hypothesized difference between the two groups of 16 (considered to be biologically significant), and the same standard deviation in both groups (DS = 13 unities) (6 rabbits, 2 implants per leg, 2 legs per rabbit, n = 12 for each surface, n = 24 total).

For each implant, the mean and SD were calculated for all continuous histomorphometric parameters. The association between two continuous variables of different groups was tested by independent Student's t-test. The Pearson chi-square test was used for the comparison of discrete variables. A two-tailed *p*-value equal to or less than 0.05 was

considered significant. The arithmetical mean for the variables Ra, Rt, and Rz of each implant system was calculated, and Fisher's exact test was applied.

To measure the agreement for the repeated measurements of ISQ values, the root mean squared values and the intraclass classification coefficient (ICC) were calculated. In terms of ICC, the values were 0.98 and 0.96 for the initial and final ISQ values, respectively, which indicate excellent agreement. A parametric two-way ANOVA analysis was conducted to compare two types of RFA devices for both implants at the two times that were measured (surgery versus sacrifice). Data analysis was performed with statistical software (SPSS for Windows 18.0; SPSS Inc., Chicago, IL, USA) with a 5% significance level.

3. Results

3.1. Surface Characterization

Carbon (C), oxygen (O), and nitrogen (N) were found in all the samples analyzed at a high concentration, as these are found in the air. A concentration of aluminum was observed in SB due to the residual alumina from the sand-blasting treatment (Figure 2). Moreover, these dental implants presented traces of calcium. Calcium comes from alumina contamination. These traces were removed by acid treatment in the SB + AE samples. In relation to the SB + AE samples, sulfur traces from H₂SO₄ were detected. The content was lower than 0.0005% (Figure 3). Table 1 shows the results of the chemical composition by XPS.

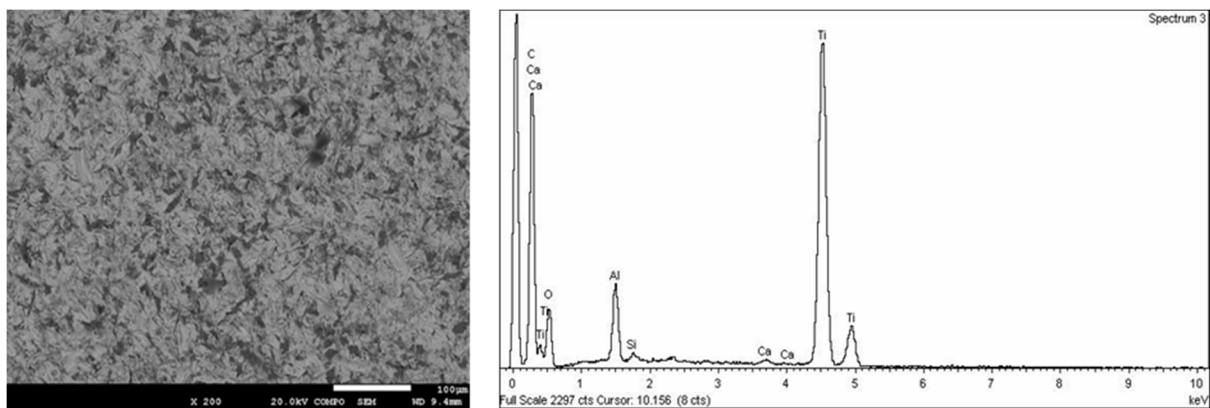


Figure 2. Surface of SB implants observed by scanning electron microscopy and X-ray microanalysis.

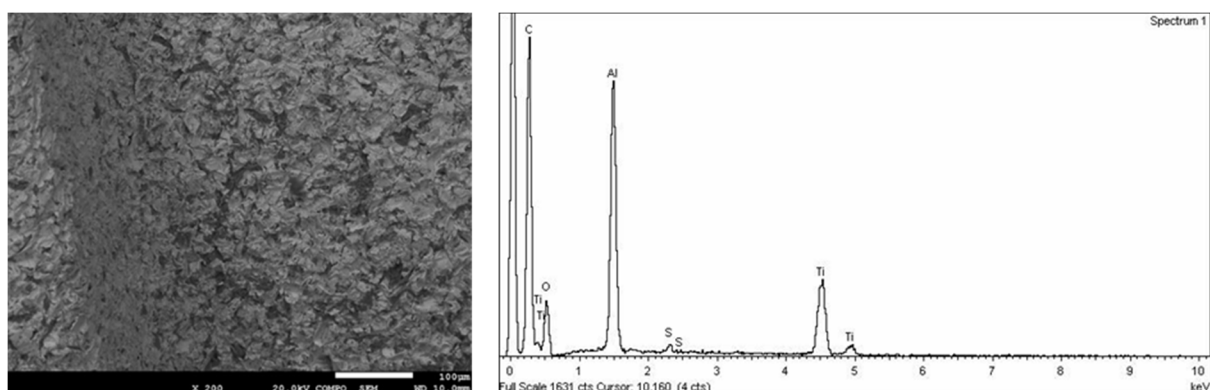


Figure 3. Surface of SB + AE implants observed by scanning electron microscopy and X-ray microanalysis.

Table 1. Weight percentage of each element detected by XPS on the implant surface. “-” means that the chemical element was not detected.

Surfaces Treatment Code	C	O	N	Ti	Al	Si	Ca	Na	Cl	Mg	P	Zn
SB	62.6	23.6	1.1	2.9	5.9	4.8	0.4	-	-	-	0.5	-
SB + AE	58.4	28.4	1.2	7.0	4.0	3.5	0.8	0.8	-	-	-	-

From the SEM observations (Figures 2 and 3) we can see that the morphology of the roughness of the peaks and valleys was very similar. The original samples before surface treatments had smooth surfaces with a roughness R_a of around 0.25 micrometers. The results can be observed in Table 2.

Table 2. Roughness measurements for the two dental implants studied. No statistically significant differences were observed in any roughness parameter.

Treatment Code	R_a (μm)	R_t (μm)	R_z (μm)
SB	2.69 ± 0.52	28.41 ± 0.24	30.52 ± 1.01
SB + AE	2.54 ± 0.61	21.66 ± 0.32	27.49 ± 0.96

The water contact angles (CA) and the calculated values for the surface free energy (SFE) and its compounds following the Owens and Wendt approach are shown in Table 3. It can be observed that SB implants increased the contact angle in comparison with SB + AE. In consequence, SB implants presented more hydrophilic behavior than SB + AE implants. This fact occurred in the three dissolvents studied.

Table 3. Apparent contact angles for the three liquids used on the different c.p. Ti surfaces. Values are mean \pm standard deviation. Statistical differences vs. smooth surfaces for each column are indicated by single asterisk symbols ($p < 0.05$).

Surface	Water CA' [$^\circ$]	Di-Iodomethane CA' [$^\circ$]	Formamide CA' [$^\circ$]
SB	74.7 ± 0.5	63.4 ± 1.5	58.2 ± 2.5
SB + AE	$64.3 \pm 0.7^*$	$47.2 \pm 1.3^*$	$45.1 \pm 1.9^*$

The results of surface energy and the dispersive and polar components are shown in Table 4. Comparing dispersive or polar components of SFE, there was a general trend in the polar component decreasing when the samples were SB (Table 4). The polar component is important, as it can facilitate the adsorption of human osteoblast precursor proteins due to the negative charge density on the surface. Statistically significant differences were found in the dispersive components between SB and SB + AE surfaces with $p < 0.05$. For the polar component the differences were $p < 0.10$.

Table 4. Surface energy (mJ/m^2) and its components for the different Ti surfaces. Values are mean \pm standard deviation. Statistical differences for each column are indicated by single-asterisk and double-asterisk symbols ($p < 0.05$).

Surface	Total	Dispersive Component	Polar Component
SB	$30.1 \pm 2.2^*$	$21.7 \pm 1.2^*$	12.5 ± 2.1
SB + AE	$39.8 \pm 2.5^{**}$	$27.8 \pm 2.6^{**}$	16.0 ± 3.4

3.2. Clinical Findings

After surgery, the six rabbits recovered fine. During the healing period, no problems with soft tissue healing nor any signs of infection in the surgical areas were seen. At the end of the experimental periods (6 weeks), all implants were found to be stable when tested.

This was verified by the torque manual and with the RFA. Therefore, the total number of implants placed was 24 (sample size for each group $n = 12$).

3.3. Histologic Findings

For both groups of surfaces, we conducted a comprehensive review of sections under the optical microscope. The implant sites consisted of a triangular cortical bone devoid of any cancellous bone. The medullary space was occupied by bone marrow tissue. All implants in the two groups appeared to be osseointegrated and showed no soft tissue encapsulation. Most bone–implant contacts were observed within the cortical areas. No major morphologic differences were seen among the two groups in the cortical bone or marrow tissues. There were areas where a clear demarcation between the original cortical bone and the new bone was visible. Figure 4 shows the histology for the SB and SB + AE surfaces.

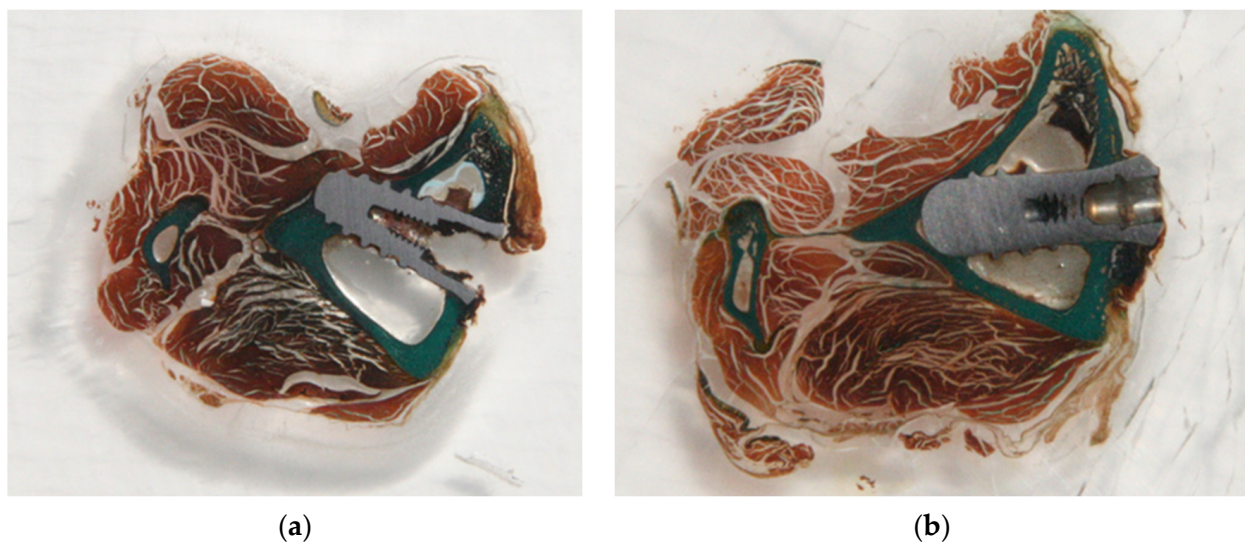


Figure 4. Histological cut of the implant section obtained by microscope: (a) SB implant; (b) SB + AE implant.

Two clearly defined different types of bones were found in the histology: an initial cortical, laminar, compact bone with the presence of osteomas, and another type of osseous forming the new bone, which was less organized, less laminar, and seemed to be in line with bone tissue.

Histologic analysis values different parameters related to osseointegration, such as the presence of fibrous tissue. Pathologists identified four categories: high, medium, medium–high, and medium–low. Most of our implants were in the medium and medium–low groups.

Upon analyzing by type of surface, we found that the shot-blasted implants were in the medium–low, medium, and medium–high groups, whereas the SB + AE fibrous tissues present were in the lower, low, medium–low, and medium groups. Another important histological parameter is the formation of trabecular bone. In this case, four categories were established: low, medium–low, medium, and medium–high. The histologic studies showed trabecular bone implants in the medium–low and medium–high groups. The study of surface type showed that the shot-blasted implants had an even distribution between different categories (low, medium–low, medium, and medium–high), whereas nine of the 12 SB + AE implants were low or medium–low.

The last important aspect in the histomorphometric analysis is the presence of new bone away from the primitive bone. Only two variables (YES/NO) were established. Two thirds of the implants showed no new bone away, whereas a third did.

3.4. Histomorphometrical Analysis

Wilcoxon's signed-rank test was conducted to determine statistically significant differences in BIC between both groups. The obtained differences were not considered significant at $p > 0.05$. So, similar BIC was observed after 6 weeks of healing both in the SB + AE implants (24.587 ± 10.54) and SB implants (21.50 ± 4.60).

Following the instructions of the pathologist and the Department of Statistics, we decided to examine the percentage of partial contact between the bone and the implant since the rabbit tibia is very spongy bone marrow. After placement of the implants, we found via histomorphometric analysis that there were locations of bone–implant contact, as described in Materials and Methods.

Comparing the SB + AE implant with SB, both showed a similar percentage of bone contact (BIC). The average percentage of partial contact between the implant and bone (p.BIC) was 55.18 ± 15.67 and 59.9 ± 13.15 for SB and SB + AE implants, respectively. In both groups, we obtained high values, and the obtained differences were not considered significant ($p = 0.05$).

3.5. ISQ Values

The measurements were made three times with both Osstell ISQ and Osstell Mentor with the specific transducer (Table 5). Mean values and standard deviations were calculated (Table 3). As described, an intraclass correlation analysis (ICC) for both devices was also conducted. With the Osstell Mentor II, the ICC after implantation was 0.902–0.977. The data obtained with Osstell ISQ on the day of the surgery were 0.911–0.979. For Osstell Mentor II after sacrifice the ICC was 0.79–0.95. The ICC with Osstell ISQ at the same time was 0.895–0.975. For the Osstell Mentor II with Osstell ISQ after the placement of the implants, the ICC was 0.980 [0.964–0.990]. The ICC for Osstell Mentor II with Osstell ISQ at necropsy was 0.961 [0.930–0.981]. This means that a correlation exists between the ICC both measurement systems (0.98) with an almost perfect degree of concordance.

Table 5. Results of ISQ values obtained by the Osstell Mentor II and Osstell ISQ systems at surgery and sacrifice time on both surfaces (SB and SB + AE).

Surfaces	Statistics	Surgery ISQ		Necropsy ISQ	
		Osstell ISQ	Osstell Mentor II	Osstell ISQ	Osstell Mentor II
SB	\bar{x}	73.72	78.08	73.72	73.77
	D.T.	6.95	7.15	6.52	6.61
SB + AE	\bar{x}	78.47	73.97	78.25	78.5
	D.T.	4.67	4.82	5.71	4.85
p-values	p value	0.62	1.13	0.84	0.59
	IC 95%	−9.7 to 0.26	−9.2 to 1.05	−9.7 to 0.66	−9.6 to 0.19

4. Discussion

Surface roughness is one of the key factors for the osseointegration of titanium dental implants. It has been suggested that the microtopography of the implant surface affects both the biological fixation and the mechanical anchoring of the implants to bone tissue. In a previous study by Buser [23], where the SB and AE surface was analyzed, the implant surface achieved the greatest amount of bone contact of five different titanium surfaces in cancellous bone after 3 and 6 weeks of healing. The present investigation evaluated the osseointegration of shot-blasted implants with/without acid etching placed in the tibiae epiphyses of rabbits, and analyzed the correlation between the BIC percentage and RFA values. Comparing the SB + AE implant with SB, both showed a similar BIC percentage (55.18 ± 15.67 and 59.9 ± 13.15 for SB and SB + AE implants, respectively). After 6 weeks of healing, there was no significant difference between SLA implants and the shot-blasted group for the ISQ values, and the ISQ values increased over time in both groups.

Moreover, it is important that the surface of an implant have a hydrophilic surface, which improves cellular anchorage and vascularization in the area, since the level of vascularization of the peri-implant tissues in the area of contact with the tissues is very poor, thus improving healing and reducing inflammation of these tissues [24–26]. In our study, the contact angle values in water were 74.7° for the SB surface and 64.3° for the SB + AE surface. According to the usual classification, both surfaces were considered hydrophilic, as the contact angle was less than 90° . However, these differences in wettability and surface energy did not have a lot of influence on the osseointegration behavior. The similar roughness seemed to be a more important characteristic than the wettability and surface energy in this case.

In addition, the XPS microanalysis of the surfaces revealed aluminum contents at both the SB and SB + AE surfaces, which means that alumina were present during the osseointegration process [27,28]. Three oxygen atoms that confronted the alumina produced a negative density on the surface that favored the selective adsorption of fibronectin, which is the precursor protein of osteoblasts. Consequently, contact angles and residual alumina favored the osseointegration. However, the total surface energy, and especially the polar component, was higher in SB + AE than in SB, and these physico-chemical properties improved the osseointegration. These beneficial and detrimental factors have been studied by several authors [10,21,22], and it has been shown that the differences between the two surfaces in relation to parameters are very important for the adsorption of key proteins in the osseointegration process, such as fibronectin, and also influence the zeta potential of the dental implant surface, which will electrostatically favor the binding of osteogenic precursor proteins.

In the current study, implants with different surface properties and the bone response to these implants were histomorphometrically analyzed in rabbits. Even though it is considered as a destructive method, histomorphometric measurement is a representative test in studying the nature of the implant–tissue surface and has been used by several authors to evaluate the bone–implant interface [29–31]. A histological evaluation of the specimens in the study showed that osseointegration was achieved for all types of implants after a healing period of 6 weeks. All implants in the two groups appeared to be osseointegrated and showed no soft tissue encapsulation. Most bone–implant contacts were observed in the cortical areas. No major morphologic differences were seen among the two groups in the cortical bone or marrow tissues.

RFA results at implant placement were $x^- 78.47$ ISQ with 4.67 deviations, similar to the results obtained by Romero et al. [32] of from 65 to 81 ISQ at surgery time for three different types of surfaces. As the literature indicates, different factors are associated with the bone–implant interface, primary stability, surgical technique, macroscopic design, and type of bone that surrounds the implant [33,34].

In the literature, we observed an evolution in the analysis resonance frequency systems. Osstell Mentor is the basis of Osstell ISQ development. As the results show, both are very reliable, but the ICC for Osstell Mentor II at both times registered was slightly less reliable. This makes us appreciate that the evolution of the device has been correct and beneficial, which decreases time because three records are not needed and the results are more reliable (almost perfect). Fontana et al. [35] carried out a similar study to ours with different surfaces, a larger sample ($n = 214$), and different times of sacrifice: 2, 4, and 9 weeks. In that study, a Ca-P surface (test) was compared to a titanium porous oxide surface (control) in terms of bone-to-implant contact (BIC) and removal torque value (RTQ) in a rabbit model. Histological analysis in terms of BIC and RTQ did not reveal any significant difference between the Ca-P oxidized surface and the oxidized surface at 2 and 4 weeks. At 9 weeks, the oxidized surface demonstrated better results in terms of RTQ in the tibiae.

Hyun-Soon Pak et al. [13] also conducted a study to investigate the bone response to dental implants with different surface characteristics using the rabbit tibia model. Tricalcium phosphate (TCP) coated, anodic oxidized, and turned (control) surfaces were compared. The results were 44.92 ± 31.87 for the TCP-coated surface, 41.41 ± 27.74 for the

anodized surface, and 25.19 ± 24.66 for the control, all being lower results those obtained in our study (59.9 ± 27.2 to 55.2 ± 42.2 SLA and for shot-blasted). This may be due to the technique used, the larger sample size, etc.

Many methods have been used to measure stability and to detect stability problems in dental implants. One of the aims of the present study was to investigate the correlation between two RFA devices currently available on the market: Osstell ISQ and Osstell Mentor. The intraclass correlation coefficient was 0.95 for both of them at day 0 and 6 weeks. The results of this study prove that the RFA system, the Osstell system, is a reliable system to measure implant stability, and thus in agreement with the results of the work by Jaramillo [15], who compared the reliability of Osstell Mentor and Osstell ISQ in an implant stability measurement, and assessed whether their measurements were comparable. Implant stability was measured with both devices on 58 implants in 15 patients. Resonance frequency analysis systems in Osstell Mentor and Osstell ISQ showed almost perfect reproducibility and repeatability.

The article published by Cho et al. [36] about the results obtained by Osstell was realized to evaluate the correlation between two generations: Osstell and Osstell Mentor. In addition, measuring the RFA effectiveness and accuracy of both devices was also carried out. In Cho's study, ISQ values were measured in 47 patients with 62 implants placed using Osstell and Osstell Mentor. The results obtained from the first phase for Osstell and Osstell Mentor were 70.84 and 75.09, respectively, with a statistically significant difference ($p < 0.01$). After that, at the second phase registration, the ISQ values of Osstell and Osstell Mentor were 71.76 and 75.94, respectively, also presenting a statistically significant difference ($p < 0.01$). The difference between the ISQ values for Osstell and Osstell Mentor at both stages was significant.

Other aspects must be taken into account in addition to osseointegration in dental implants, as indicated by Lo Giudice et al. [37]. Superficial topography of the material or coatings with low roughness and adequate homogeneity could also be related to bacterial adhesion and human cell viability. Therefore, the laboratorial and clinical modifications will affect not only the mechanical aspect of the dental materials, but also the biological response.

An important limitation of this study is that it should be extended in the future with different roughness values to confirm that it is this parameter that plays the main role. Work should also be done with the study of bacteria, as topography is also very sensitive to biofilm formation.

5. Conclusions

The main finding of our research is that both surfaces of implants showed high osseointegration obtained by resonance frequency analysis. The acid etching after the shot-blasting increase the hydrophobic character but also increased the surface energy. The two factors, wettability, which promotes osseointegration, and energy, which decreases osseointegration, offset the bone formation values. In addition, the increase in roughness caused by acid etching on the shot-blasted samples was too small to cause variations in bone colonization. The reproducibility and repeatability found between RFA in Osstell Mentor and Osstell ISQ is near-perfect.

Author Contributions: B.R.-C. assisted with the implant surgery. B.F.L. supervised the content. J.V.R.-S. designed the study. M.H.-C. was the surgeon. F.J.G.M. conducted the histomorphometric analysis. All authors have read and agreed to the published version of the manuscript.

Funding: The authors would like to thank SOADCO (Escaldes-Engordany, Andorra) for the financial support provided.

Institutional Review Board Statement: The study was conducted according to the guidelines of the Declaration of Helsinki, and approved by the Ethics Committee of Universidad de Cordoba- Facultad de Veterinaria (protocol code 2041/PI11 and date of approval 11 November 2019).

Informed Consent Statement: Not applicable.

Data Availability Statement: Not applicable.

Acknowledgments: The authors are grateful to Klockner dental implants for donating the samples. This research was funded by the Spanish Government and European Union FEDER via concession of the grant RTI2018-098075-B-C22, and the research group Generalitat de Catalunya 2017SGR708.

Conflicts of Interest: The authors declare no conflict of interest.

References

1. Brånemark, P.I.; Hansson, B.O.; Adell, R.; Breine, U.; Lindström, J.; Hallén, O.; Ohman, A. Osseointegrated implants in the treatment of the edentulous jaw. Experience from a 10-year period. *Scand. J. Plast. Reconstr. Surg. Suppl.* **1977**, *16*, 1–132.
2. Albrektsson, T.; Brånemark, P.-I.; Hansson, H.-A.; Lindström, J. Osseointegrated Titanium Implants: Requirements for Ensuring a Long-Lasting, Direct Bone-to-Implant Anchorage in Man. *Acta Orthop. Scand.* **1981**, *52*, 155–170. [[CrossRef](#)] [[PubMed](#)]
3. Davies, J.E.; Houssein, M.M. Bone Formation and Healing: Histodynamics of endosseous Wound Healing. In *Bone Engineering*; Davies, J.E., Ed.; Springer: London, UK, 1999; pp. 1–15.
4. Le Guehennec, L.; Soueidan, A.; Layrolle, P.; Amouriq, Y. Surface treatments of titanium dental implants for rapid osseointegration. *Dent. Mater.* **2007**, *23*, 844–854. [[CrossRef](#)] [[PubMed](#)]
5. El Hassanin, A.; Quaremba, G.; Sammartino, P.; Adamo, D.; Miniello, A.; Marenzi, G. Effect of Implant Surface Roughness and Macro- and Micro-Structural Composition on Wear and Metal Particles Released. *Materials* **2021**, *14*, 6800. [[CrossRef](#)]
6. Marenzi, G.; Impero, F.; Scherillo, F.; Sammartino, J.C.; Squillace, A.; Spagnuolo, G. Effect of Different Surface Treatments on Titanium Dental Implant Micro-Morphology. *Materials* **2019**, *12*, 733. [[CrossRef](#)]
7. Matos, G.R.M. Surface Roughness of Dental Implant and Osseointegration. *J. Maxillofac. Oral Surg.* **2021**, *20*, 1–4. [[CrossRef](#)]
8. Lee, J.K.; Choi, D.-S.; Jang, I.; Choi, W.-Y. Improved osseointegration of dental titanium implants by TiO₂ nanotube arrays with recombinant human bone morphogenetic protein-2: A pilot in vivo study. *Int. J. Nanomed.* **2015**, *10*, 1145–1154.
9. Lee, H.-J.; Yang, I.-H.; Kim, S.-K.; Yeo, I.-S.; Kwon, T.-K. In vivo comparison between the effects of chemically modified hydrophilic and anodically oxidized titanium surfaces on initial bone healing. *J. Periodontal Implant. Sci.* **2015**, *45*, 94–100. [[CrossRef](#)]
10. Aparicio, C.; Rodriguez, D.; Gil, F.J. Variation of roughness and adhesion strength of deposited apatite layers on titanium dental implants. *Mater. Sci. Eng. C* **2011**, *31*, 320–324. [[CrossRef](#)]
11. Von Wilmowsky, C.; Moest, T.; Nkenke, E.; Stelzle, F.; Schlegel, K.A. Implants in bone: Part I. A current overview about tissue response, surface modifications and future perspectives. *Oral Maxillofac. Surg.* **2013**, *18*, 243–257. [[CrossRef](#)]
12. Albertini, M.; Yagüe, M.F.; Lazaro, P.; Herrero-Climent, M.; Ríos-Santos, J.; Bullon, P.; Gil, F. Advances in surfaces and osseointegration in implantology. Biomimetic surfaces. *Med. Oral Patol. Oral Cir. Bucal* **2015**, *20*, e316–e325. [[CrossRef](#)]
13. Pak, H.-S.; Yeo, I.-S.; Yang, J.-H. A histomorphometric study of dental implants with different surface characteristics. *J. Adv. Prosthodont.* **2010**, *2*, 142–147. [[CrossRef](#)]
14. Albrektsson, T.; Wenneberg, A. Oral implant surfaces: Part 1- review focusing on topographic and chemical properties of different surfaces and in vivo responses to them. *Int. J. Prosthodont.* **2004**, *17*, 536–543.
15. Ferraz, E.P.; Sverzut, A.T.; Freitas, G.P.; Alves, C., Jr.; Beloti, M.M.; Rosa, A.L. Bone tissue response to plasma-nitrided titanium implant surfaces. *J. Appl. Oral Sci.* **2015**, *23*, 9–13. [[CrossRef](#)] [[PubMed](#)]
16. Meredith, N.; Alleyne, D.; Cawley, P. Quantitative determination of the stability of the implant-tissue interface using resonance frequency analysis. *Clin. Oral Implant. Res.* **1996**, *7*, 261–267. [[CrossRef](#)] [[PubMed](#)]
17. Geckili, O.; Cilingir, A.; Bural, C.; Bilmenoglu, C.; Bilhan, H. Determination of the Optimum Torque to Tighten the Smartpegs of Magnetic Resonance Frequency Analyses Devices: An Ex Vivo Study. *J. Oral Implant.* **2015**, *41*, e252–e256. [[CrossRef](#)]
18. Jaramillo, R.; Santos, R.; Lazaro, P.; Romero, M.; Rios-Santos, J.V.; Bullon, P.; Fernandez-Palacin, A.; Herrero-Climent, M. Comparative Analysis of 2 Resonance Frequency Measurement Devices: Osstell Mentor and Osstell ISQ. *Implant Dent.* **2014**, *23*, 1–6. [[CrossRef](#)]
19. Sennerby, L.; Pagliani, L.; Petersson, A.; Verrocchi, D.; Volpe, S.; Andersson, P. Two different implant designs and impact of related drilling protocols on primary stability in different bone densities: An in vitro comparison study. *Int. J. Oral Maxillofac. Implant.* **2015**, *30*, 564–568. [[CrossRef](#)]
20. Huang, H.-L.; Tsai, M.-T.; Su, K.-C.; Li, Y.-F.; Hsu, J.-T.; Chang, C.-H.; Fuh, L.-J.; Wu, A.Y.-J. Relation between initial implant stability quotient and bone-implant contact percentage: An in vitro model study. *Oral Surg. Oral Med. Oral Pathol. Oral Radiol.* **2013**, *116*, e356–e361. [[CrossRef](#)]
21. Sharma, P.; Rao, K.H. Analysis of different approaches for evaluation of surface energy of microbial cells by contact angle goniometry. *Adv. Colloid Interface Sci.* **2002**, *98*, 341–463. [[CrossRef](#)]
22. Pegueroles, M.; Gil, F.; Planell, J.; Aparicio, C. The influence of blasting and sterilization on static and time-related wettability and surface-energy properties of titanium surfaces. *Surf. Coat. Technol.* **2008**, *202*, 3470–3479. [[CrossRef](#)]
23. Buser, D.; Schenk, R.K.; Steinemann, S.; Fiorellini, J.P.; Fox, C.H.; Stich, H. Influence of surface characteristics on bone integration of titanium implants. A histomorphometric study in miniature pigs. *J. Biomed. Mater. Res.* **1991**, *25*, 889–902. [[CrossRef](#)]
24. Ström, G.; Fredriksson, M.; Stenius, P. Contact angles, work of adhesion, and interfacial tensions at a dissolving Hydrocarbon surface. *J. Colloid Interface Sci.* **1987**, *119*, 352–361. [[CrossRef](#)]

25. Shin, Y.; Akao, M. Tissue Reactions to Various Percutaneous Materials with Different Surface Properties and Structures. *Artif. Organs* **2008**, *21*, 995–1001. [[CrossRef](#)] [[PubMed](#)]
26. Quarles, L.D.; Wenstrup, R.J.; Castillo, S.A.; Drezner, M.K. Aluminum induced mitogenesis in MC3T3-E1 osteoblasts: Potential mechanism underlying neoosteogenesis. *Endocrinology* **1991**, *128*, 3144–3151. [[CrossRef](#)]
27. Lau, K.H.; Yoo, A.; Wang, S.P. Aluminum stimulates the proliferation and differentiation of osteoblasts in vitro by a mechanism that is different from fluorine. *Mol. Cell Biochem.* **1991**, *105*, 93–105. [[PubMed](#)]
28. Johansson, C.; Albrektsson, T. Integration of screw implants in the rabbit: A 1-year follow-up of removal torque of titanium implants. *Int. J. Oral Maxillofac. Implant.* **1987**, *2*, 69–75.
29. Herrero-Climent, M.; Santos-Garcia, R.; Jaramillo-Santos, R.; Romero-Ruiz, M.; Fernández-Palacín, A.; Lazaro-Calvo, P.; Bullon, P.; Ríos-Santos, J. Assessment of osstell isq's reliability for implant stability measurement: A cross-sectional clinical study. *Med. Oral Patol. Oral Cir. Bucal* **2013**, *18*, e877–e882. [[CrossRef](#)] [[PubMed](#)]
30. Meredith, N. Assessment of implant stability as a prognostic determinant. *Int. J. Prosthodont.* **1998**, *11*, 491–501.
31. Aparicio, C.; Padrós, A.; Gil, F.-J. In vivo evaluation of micro-rough and bioactive titanium dental implants using histometry and pull-out tests. *J. Mech. Behav. Biomed. Mater.* **2011**, *4*, 1672–1682. [[CrossRef](#)]
32. Romero-Ruiz, M.M.; Gil-Mur, F.J.; Ríos-Santos, J.V.; Lázaro-Calvo, P.; Ríos-Carrasco, B.; Herrero-Climent, M. Influence of a Novel Surface of Bioactive Implants on Osseointegration: A Comparative and Histomorfometric Correlation and Implant Stability Study in Minipigs. *Int. J. Mol. Sci.* **2019**, *20*, 2307. [[CrossRef](#)] [[PubMed](#)]
33. Diaz-Castro, M.; Falcao, A.; Lopez-Jarana, P.; Falcao, C.; Rios-Santos, J.; Fernandez-Palacin, A.; Herrero-Climent, M. Repeatability of the resonance frequency analysis values in implants with a new technology. *Med. Oral Patol. Oral y Cir. Bucal* **2019**, *24*, e636–e642. [[CrossRef](#)] [[PubMed](#)]
34. Simmons, D.E.; Maney, P.; Teitelbaum, A.G.; Billiot, S.; Popat, L.J.; Palaiologou, A.A. Comparative evaluation of the stability of two different dental implant designs and surgical protocols—A pilot study. *Int. J. Implant. Dent.* **2017**, *3*, 16. [[CrossRef](#)] [[PubMed](#)]
35. Fontana, F.; Rocchietta, I.; Addis, A.; Schupbach, P.; Zanotti, G.; Simion, M. Effects of a calcium phosphate coating on the osseointegration of endosseous implants in a rabbit model. *Clin. Oral Implant. Res.* **2010**, *22*, 760–766. [[CrossRef](#)]
36. Cho, I.-H.; Lee, Y.-I.; Kim, Y.-M. A comparative study on the accuracy of the devices for measuring the implant stability. *J. Adv. Prosthodont.* **2009**, *1*, 124. [[CrossRef](#)]
37. Lo Giudice, R.; Tribst, J.P.M. Dental Materials Coatings:Effect on the clinical behavior. *Coatings* **2020**, *10*, 1229. [[CrossRef](#)]